Journal of Alloys and Compounds, 207/208 (1994) 206–212
JALCOM 3096

Phase diagram and phase separation in $La_{2-x}Sr_xCuO_{4+\delta}$

D.C. Johnston, F. Borsa, J.H. Cho, F.C. Chou, D.R. Torgeson, D. Vaknin, J.L. Zarestky and J. Ziolo
Ames Laboratory-US DOE and Department of Physics and Astronomy, Iowa State University, Ames, IA 50011 (USA)

J.D. Jorgensen, P.G. Radaelli, A.J. Schultz and J.L. Wagner
Argonne National Laboratory, Argonne, IL 60439 (USA)

S.-W. Cheong
AT&T Bell Laboratories, Murray Hill, NJ 07974 (USA)

Abstract

The phase diagram of the title system is remarkably rich, exhibiting regions of long-range antiferromagnetic order, short-range (spin-glass-like) order, high temperature superconductivity, or none of these. Here, the phase diagram is reviewed, with an emphasis on our recent studies using ^{139}La NQR, powder and single crystal neutron diffraction, and magnetization measurements for $0 \leqslant x \leqslant 0.15$ and $0 \leqslant \delta \lesssim 0.1$.

1. Introduction

The subject of phase separation in the high superconducting transition temperature (T_c) cuprate system $La_{2-x}Sr_xCuO_{4+\delta}$ has an interesting history. Upon subjecting La_2CuO_4 to O_2 gas at a pressure of 0.1–3 kbar and temperature $T \approx 575$–800 °C followed by furnace cooling, a bulk superconductor $La_2CuO_{4+\delta}$ is formed [1] containing $\delta \approx 0.03$ excess bulk oxygen [2–4]. This material was subsequently found to exhibit macroscopic phase separation below $T_s \sim 260$–320 K into oxygen-rich $La_2CuO_{4+\delta'}$ ($\delta' \approx 0.08$), which becomes superconducting below $T_c \approx 35$ K, and insulating antiferromagnetic (AF) $La_2CuO_{4+\delta''} \approx 0.00$) with Néel temperature $T_N \approx 250$ K $\sim T_s$ [2,4–11]. This observation of phase separation proved, surprisingly, that the excess oxygen atoms have a relatively high mobility even at room temperature. Diffraction linewidth analysis of powder samples indicated that the linear size of the phase-separated oxygen-rich regions is on the order of 3000 Å or larger, whereas the oxygen deficient phase showed no particle-size broadening of the diffraction peaks [2]. One signature of phase separation in a particular sample is the observation of both superconductivity below ≈ 35 K and AF ordering in the sample.

The lattice positions of the excess oxygens in the superconducting oxygen-rich low-temperature phase $La_2CuO_{4+\delta'}$ have been determined from single crystal neutron diffraction measurements to be located between adjacent LaO layers, tetrahedrally coordinated by four La atoms [12].

The small amount of excess oxygen and the presence of phase separation in the above $La_2CuO_{4+\delta}$ samples have been serious obstacles to determining the detailed crystal structure of the superconducting compound including the precise location(s) of the excess oxygen atoms. Recently, Wattiaux *et al.* [13] discovered that polycrystalline La_2CuO_4 can be electrochemically oxidized to much higher levels at room temperature in aqueous base, yielding [14–18] $La_2CuO_{4+\delta}$ with $0 \leqslant \delta \lesssim 0.1$.

Theoretical studies of doped holes in the CuO_2 planes of the cuprates have predicted phase separation to occur into no-hole and hole-rich phases, similar to that below T_s in $La_2CuO_{4+\delta}$ (see, *e.g.* [19]); according to one such mechanism, the doped-hole segregation occurs because the decrease in overall exchange energy between the Cu^{2+} magnetic moments arising from the hole segregation outweighs the increase in kinetic energy of the inhomogeneous hole distribution [19].

In the absence of excess oxygen, macroscopic phase separation at low (Sr) doping levels of the type seen in $La_2CuO_{4+\delta}$ below ≈ 300 K has not been observed in $La_{2-x}Sr_xCuO_4$, even though the above theoretical predictions suggest that such phase separation should occur. This is presumably because the Sr^{2+} ions are not mobile and cannot phase-separate along with the doped holes, so that the phase separation is "frustrated"

SSDI 0925-8388(94)03096-F

[20]. In the following, some highlights of our recent studies on the magnetic and structural phase diagrams of both $La_2CuO_{4+\delta}$ and $La_{2-x}Sr_xCuO_{4+\delta}$, in the doping ranges $0 \leqslant x \leqslant 0.15$ and $0 \leqslant \delta \lesssim 0.1$, are reviewed.

2.1. The $La_2CuO_{4+\delta}$ system

In order to understand the relationships between the phase separation below T_s and antiferromagnetic (AF) ordering below T_N, a simultaneous structural and magnetic neutron diffraction study was carried out on a single crystal of $La_2CuO_{4+\delta}$ with $\delta \approx 0.03$ [21]. The crystal was synthesized by subjecting a conventionally prepared La_2CuO_4 crystal to O_2 gas at 3 kbar pressure at 575 °C. The data showed that T_s (≈ 260 K) was about 15 K higher than T_N.

Extensive measurements were also carried out on samples of $La_2CuO_{4+\delta}$ obtained by electrochemical oxidation of La_2CuO_4 in aqueous base at room temperature [18,22]. Two distinct ranges of T_c were observed in these samples at ~32 K and 40–45 K, with the lower T_c being found in samples with lower oxygen content. With increasing δ, a single $T_c \approx 34$ K is observed up to $\delta \approx 0.07$ as shown in Fig. 1(a). The peak in the normal state magnetic susceptibility, $\chi(T)$, near $T_N \approx 250$ K, due to the AF phase with $\delta'' \approx 0.00$, decreases with increasing δ and disappears by $\delta \sim 0.07$ as shown in Fig. 1(b). These data indicate that the miscibility gap ends by $\delta \approx 0.07$. Increasing δ to 0.11 causes T_c to increase to the range 40–45 K, as shown in Fig. 2; intermediate compositions show both $T_c \approx 32$ K and $T_c \sim 40$–45 K. This observation suggests that two chemically and/or structurally distinct phases are present at low temperature at $\delta \approx 0.07$ and $\delta \sim 0.11$, with a two-phase region in between. Neutron diffraction structure measurements on powders with $\delta \approx 0.08$ ($T_c = 32$ K) and $\delta \approx 0.12$ ($T_c \approx 42$ K) and a single crystal with $\delta \sim 0.1$ ($T_c = 40$ K) showed that these compositions remain single phase down to 10–16 K, with no evidence for phase separation [23], confirming that these compositions are beyond the miscibility gap in the phase diagram. These structural data showed that the excess oxygen atoms are located between the two LaO layers in the unit cell, as found previously for the oxygen-rich phase in $La_2CuO_{4.03}$ [12], and that the crystallographic space group is *Fmmm*. A comparison of iodometric titration measurements and TGA measurements of the oxygen contents of electrochemically prepared $La_2CuO_{4+\delta}$ suggest that a significant amount of oxygen–oxygen bonding occurs involving the excess oxygen atoms [18,23]. Electron diffraction measurements [15–17,24] and the neutron diffraction structural studies [23] showed a long-period superstructure both parallel and perpendicular to the CuO_2 planes, presumably associated with oxygen ordering. It is not yet clear what structural features distinguish the phase with $T_c \approx 32$ K from that with $T_c \gtrsim 40$ K.

The normal state $\chi(T)$ data for polycrystalline $La_2CuO_{4+\delta}$ with $\delta = 0.11$ ($T_c \approx 45$ K) and $\delta = 0.065$ ($T_c = 32$ K), prepared using electrochemical oxidation, are plotted in Fig. 3, and compared with those of conventionally prepared $La_{1.95}Sr_{0.15}CuO_4$ ($T_c \approx 38$ K)

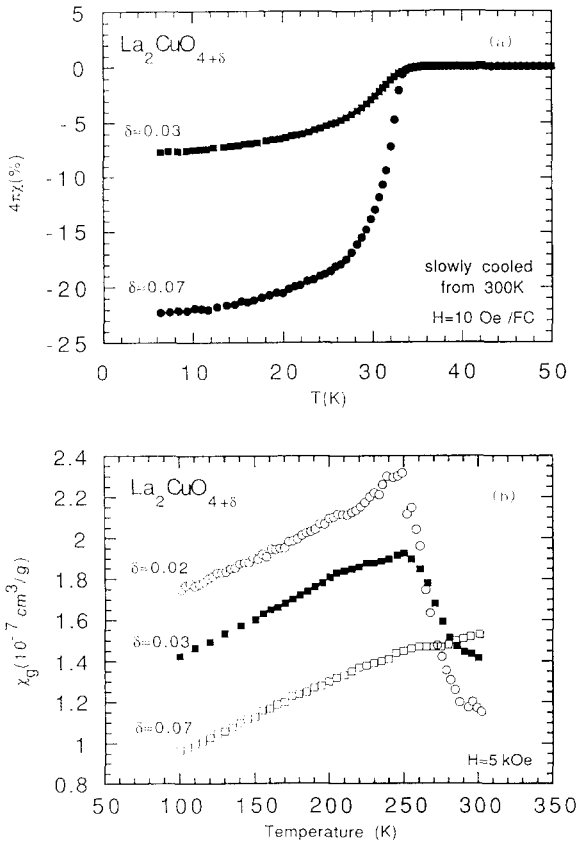

Fig. 1. Meissner fraction ($-4\pi\chi$) (a) and normal state magnetic susceptibility χ_g (b) versus temperature for $La_2CuO_{4+\delta}$ samples with $0.02 \leqslant \delta \leqslant 0.07$ [18,22].

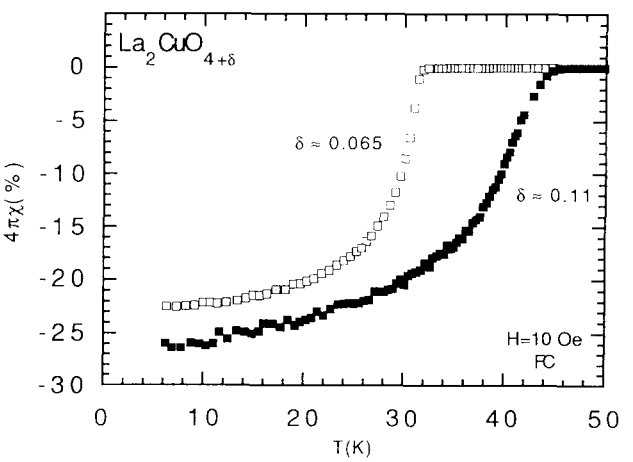

Fig. 2. Meissner fraction ($-4\pi\chi$) data for two $La_2CuO_{4+\delta}$ samples with $\delta = 0.065$ and 0.11 [22].

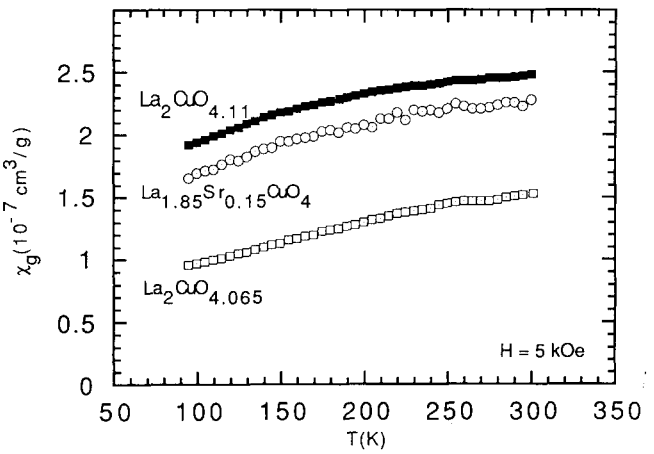

Fig. 3. Magnetic susceptibility χ_g versus temperature T for $La_2CuO_{4+\delta}$ samples with $\delta = 0.065$ and 0.11. $\chi_g(T)$ data for conventionally prepared ceramic $La_{1.85}Sr_{0.15}CuO_4$ are included for comparison [18,22].

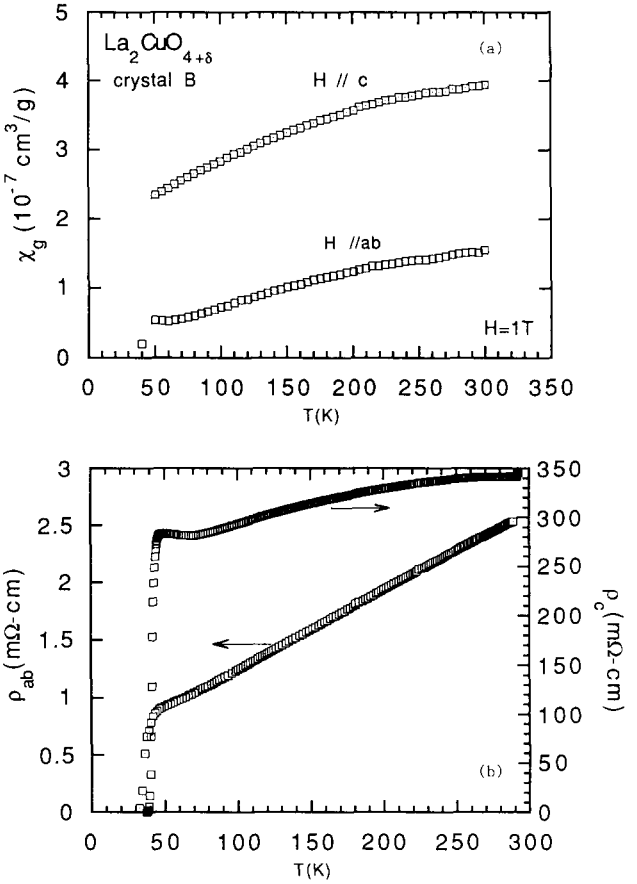

Fig. 4. Anisotropic magnetic susceptibility χ_g (a) and electrical resistivity ρ (b) versus temperature T for a single crystal of $La_2CuO_{4+\delta}$ with $\delta \approx 0.1$ [22].

[18,22]. The $\chi(T)$ data for $La_2CuO_{4.11}$ and $La_{1.85}Sr_{0.15}CuO_4$ are nearly identical, suggesting that the hole concentrations (p) in the CuO_2 planes are nearly the same. This inference is supported by iodometric titration results for these two samples, which show $p \approx 0.16$ and $p \approx 0.14$, respectively [18,23]. Anisotropic $\chi(T)$ and resistivity data for a single crystal of $La_2CuO_{4+\delta}$ with $T_c \approx 40$ K are shown in Figs. 4(a) and (b), respectively [22]. The data in Fig. 4(a) show no evidence for a peak near 250 K, indicating (see Fig. 1(b)) that homogeneous millimeter-sized $La_2CuO_{4+\delta}$ crystals can be produced using the room temperature electrochemical oxidation technique.

2.2. The $La_{2-x}Sr_xCuO_{4+\delta}$ system

2.2.1. The Néel-ordered regime: $0 \leqslant x \leqslant 0.02$

We recently reported a study with high resolution in x of the magnetic and structural phase diagram of $La_{2-x}Sr_xCuO_{4+\delta}$ in the low doping regime $0 \leqslant (x,\delta) \leqslant 0.03$, where doped holes are produced by Sr-doping and/or doping with excess oxygen [25]. Three series of $La_{2-x}Sr_xCuO_{4+\delta}$ samples were prepared by conventional solid state reaction at 1050 °C, followed by treating at 650 °C for 5 h in 1 bar N_2 or in 1 bar O_2, or at 500 °C for 72 h in 230 bar O_2, respectively, and then oven-cooled, resulting in $\delta = 0.00$, 0.01 and 0.03, respectively.

Figure 5(a) shows $\chi(T)$ data ($H = 5$ kG) for the $La_{2-x}Sr_xCuO_{4+\delta}$ samples annealed in 1 bar O_2. The downturns in the data below ≈ 40 K result from the onset of superconductivity (see below). The $\chi(T)$ data for the other two series of samples (not shown) are similar, except that the series annealed under 1 bar N_2 showed no trace of superconductivity for any of the samples. T_N is the temperature of the peak in $\chi(T)$ [26]. The T_N values are plotted versus x in Fig. 6(a) for the three series of samples. For each series, T_N decreases to ~0 K by $x \approx 0.02$. Also plotted in Fig. 6(a) is the tetragonal-to-orthorhombic transition temperature $T_{O/T}(x)$ for the three series. $T_{O/T}$ is seen to be very sensitive to δ, as observed previously for $La_2CuO_{4+\delta}$ [27]; the data for the 1 bar N_2 annealed series are in agreement with previous reports [28].

As noted above, the 1 bar N_2 annealed series $La_{2-x}Sr_xCuO_{4+\delta}$ ($\delta \approx 0$) showed no evidence of superconductivity above 5 K, confirming that macroscopic phase separation does not occur for $\delta = 0$. This result is in contrast to the behavior of the 1 bar and 230 bar O_2 annealed series ($\delta \approx 0.01$ and 0.03, respectively), which do exhibit superconductivity. $T_c(x)$ and the Meissner fraction ($-4\pi\chi$) versus x for the 230 bar O_2 annealed series ($\delta \approx 0.03$) are shown in Fig. 6(b). T_c decreases linearly with x, but is non-zero (≈ 20 K) as the Meissner fraction approaches zero at $x \approx 0.03$. For $\delta \approx 0.03$, the authors therefore concluded that the known phase separation for $x = 0$, which produces the oxygen-rich superconducting phase, no longer occurs above $x \approx 0.03$.

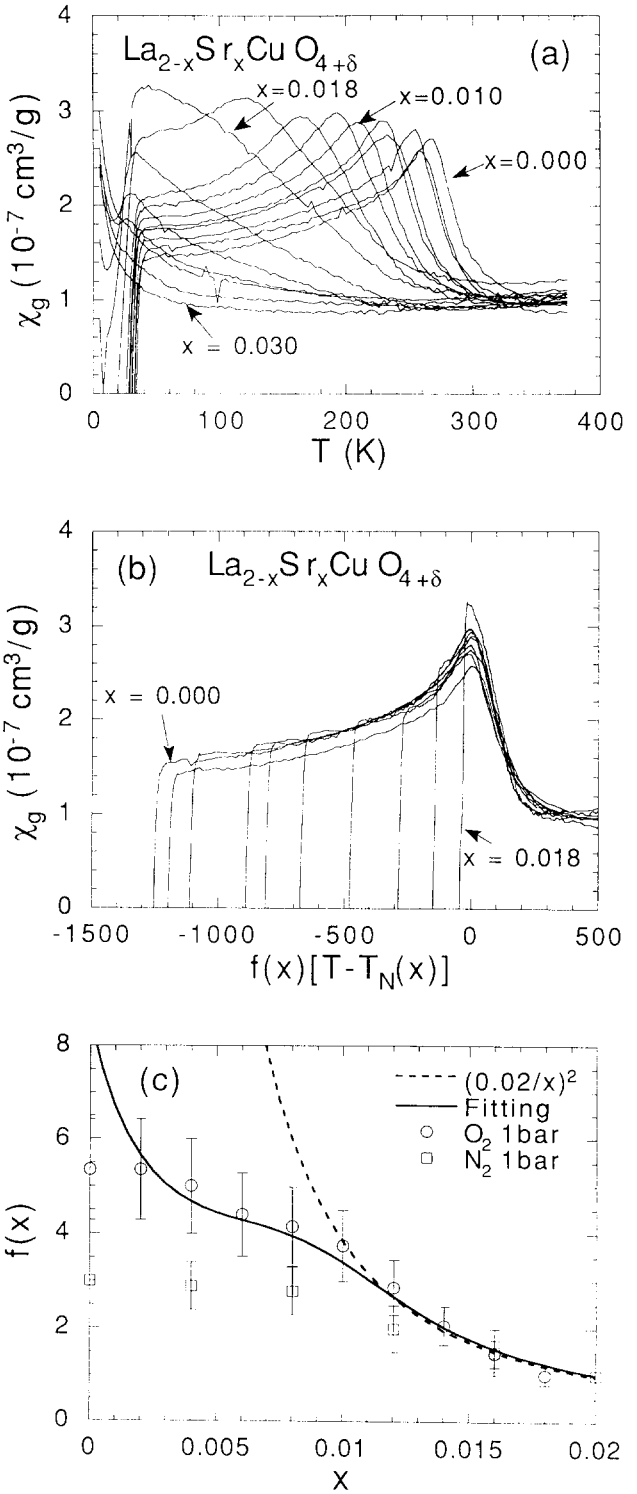

Fig. 5. (a) Magnetic susceptibility χ_g versus temperature T for the series of $La_{2-x}Sr_xCuO_{4+\delta}$ samples annealed in 1 bar O_2 ($\delta \approx 0.01$) [25]. (b) The $\chi_g(T)$ data in (a), plotted versus a reduced temperature scale as discussed in the text [25]. (c) The scaling function $f(x)$ in the abscissa in (b) [25].

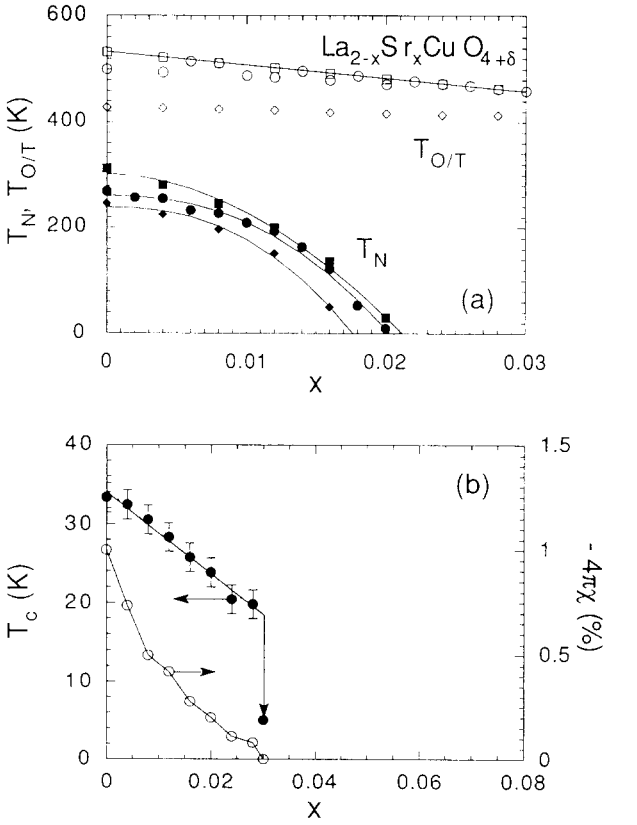

Fig. 6. (a) Dependence of the tetragonal-to-orthorhombic transition temperature $T_{O/T}$ and Néel temperature T_N on composition x for three series of $La_{2-x}Sr_xCuO_{4+\delta}$ samples annealed in 1 bar N_2 (squares, $\delta \approx 0.00$), 1 bar O_2 (circles, $\delta \approx 0.01$), and 230 bar O_2 (diamonds, $\delta \approx 0.03$) [25]. (b) Superconducting transition onset temperature (T_c) and Meissner fraction ($-4\pi\chi$) versus composition x for the series of $La_{2-x}Sr_xCuO_{4+\delta}$ samples annealed in 230 bar O_2 ($\delta \approx 0.03$) [25].

For each series, the $T_N(x)$ data in Fig. 6(a) for the AF phase $La_{2-x}Sr_xCuO_{4+\delta'}$ ($0 \leqslant x \lesssim 0.02$, $\delta' \approx 0.00$) can be fitted with $n \approx 2$ in the expression

$$1 - T_N(x)/T_N(0) = (x/x_c)^n \qquad (1)$$

where the least square fits are shown as the solid curves in Fig. 6(a). The authors noted that the power law dependence in eqn. (1) is expected from finite size scaling theory, which predicts that the measured T_N is limited by the finite size (linear dimension L) of a system. In particular, this theory predicts

$$1 - T_N(L)/T_N(\infty) \propto L^{-1/\nu} \qquad (2)$$

where in mean field theory, the exponent $\nu = 1/2$. Equations (1) and (2) are consistent, with $L(x) \propto 1/x^{n\nu}$. This consistency was interpreted to mean that the doped holes form walls separating domains of undoped material (see also below), where the magnetic coupling between domains is much weaker than within a domain. Mean field theory was argued to hold in the present case, because the long-range AF order below T_N results from weak coupling between strongly short-range AF-ordered

CuO_2 planes. Since $n \approx 2$ from above and $\nu = 1/2$, one obtains $L(x) \propto 1/x$. This dependence $L(x) \propto 1/x$ indicates that the width of a wall is independent of x.

We return now to the $\chi(T)$ data in Fig. 5(a). The peak associated with the canted AF ordering in $La_{2-x}Sr_xCuO_{4+\delta''}$ becomes broadened, as well as depressed in temperature, with increasing Sr-doping x. At the same time, the height of the peak is almost independent of x. Since the χ of the superconducting phase above T_c has a much weaker T dependence than the χ of the AF phase, this suggests that the $\chi(T)$ data for all compositions $0 \leqslant x \lesssim 0.02$ of the AF phase follow a scaling relationship

$$\chi(x, T) = \chi\{f(x)[T - T_N(x)]\} \quad (3)$$

This scaling is indeed obeyed well both above and below T_N as shown in Fig. 5(b), where the data in Fig. 5(a) for all samples collapse onto a single curve obeying eqn. (3) (except for the data associated with the superconducting phase at the lowest T). The $\chi(T)$ data for the 1 bar N_2 annealed series of samples can be scaled equally well in the same way (not shown). The scaling functions $f(x)$ for these two series are shown in Fig. 5(c). Above $x \approx 0.01$, $f(x) \propto 1/x^2$ as shown by the dashed line in Fig. 5(c). Analysis of this $f(x)$ yielded $L(x) \propto 1/x$, consistent with the $L(x)$ inferred above from analysis of $T_N(x)$. As shown by Cho *et al.* [25], the saturation of $f(x)$ in Fig. 5(c) below $x \approx 0.01$ can be qualitatively understood as arising from the T dependence of the two-dimensional AF correlation length $\xi(T)$ inferred from inelastic neutron scattering measurements, where $L(x) \equiv \xi(T = 0, x)$. The solid curve in Fig. 5(c) is the resulting theoretical fit to the $f(x)$ data for the 1 bar O_2 annealed series of samples.

From the above work, Cho *et al.* [25] concluded that the doped holes in the AF phase $La_{2-x}Sr_xCuO_{4+\delta''}$ ($0 \leqslant x \lesssim 0.02$, $\delta'' \approx 0.00$) condense into walls separating microscopic undoped domains, producing an electronically and magnetically inhomogeneous state, as predicted theoretically [19,20]. This novel doping-induced finite-size effect provides a natural physical basis for understanding the anomalously strong depression of T_N and the strong reduction of the zero-temperature ordered magnetic moment in the AF phase with hole doping [28].

The above studies of $T_N(x)$ and $\chi(x, T)$ were carried out at temperatures above about 50 K, where the doped holes are delocalized. Chou *et al.* [29] have performed extensive ^{139}La NQR measurements to lower temperatures. These data provide atomic-scale evidence for localization of the doped holes' charge below ~30 K [29]. The most dramatic effect observed in the ^{139}La NQR in $La_{2-x}Sr_xCuO_4$ for $x \leqslant 0.02$ below ~20 K is in the temperature dependence of the nuclear-spin-lattice relaxation rate (NSLRR), R_1, shown in Fig. 7 [29]. The

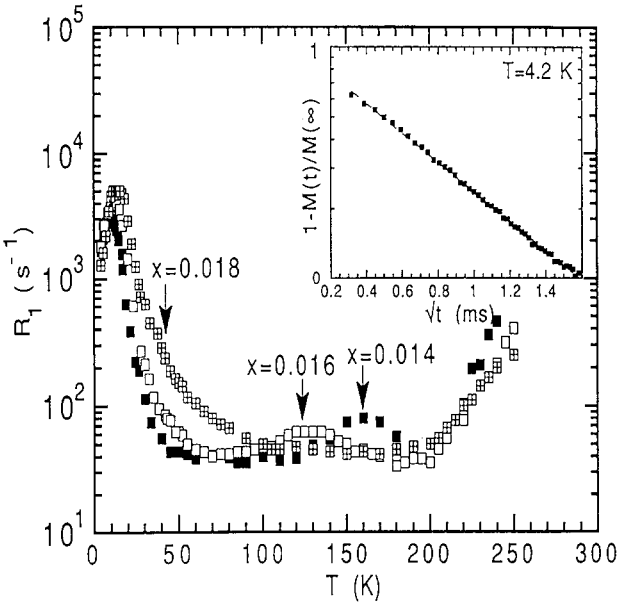

Fig. 7. Nuclear spin-lattice relaxation rate (R_1) for the $2\nu_Q$ ^{139}La NQR transition versus temperature T for several of the samples in the $La_{2-x}Sr_xCuO_{4+\delta}$ series annealed in 1 bar O_2 ($\delta \approx 0.01$) [29]. The vertical arrows denote the T_N values for the respective samples. Inset: Recovery of the nuclear magnetization $M(t)$ versus $\sqrt{t}$ for $x = 0.018$.

data exhibit a weak peak associated with the long-range AF ordering at the same T_N as obtained from $\chi(T)$ results. In addition, R_1 displays a strong peak at a temperature $T_f < 16$ K, where $T_f \propto x$. The authors identified T_f as the freezing temperature of the spin degrees of freedom associated with the doped holes. It was not clear from the NQR data whether a true phase transition or a continuous spin freezing occurs at T_f.

As shown in Fig. 8 [29], T_f is proportional to x with a large slope: $T_f = (815\ \text{K})x$. In the context of known re-entrant or conventional spin glasses, both features are remarkable. In Fig. 8, there is no discernible threshold in x for freezing of the doped hole spins, in contrast to the usual case where a percolation threshold must first be exceeded.

2.2.2. The spin-glass-like regime $0.02 \leqslant 0.08$

From ^{139}La NQR measurements, Cho *et al.* [30] found strong peaks in the NSLRR below 10 K, similar to but sharper than those shown for $x \leqslant 0.02$ in Fig. 7. The spin glass ordering temperatures (T_g), defined as the temperatures of the peaks in the NSLRR, are plotted in Fig. 8. Analysis of the NQR data indicated that the transition at T_g is associated with the freezing of dynamically well-ordered undoped domains separated by walls of hole-rich material. Both the NQR [30] and neutron scattering [31] investigations found $L(x) \propto x^{-1/2}$, indicating that a crossover occurs in $L(x)$ from $L(x) \propto 1/x$ for $x < 0.02$ to $L(x) \propto 1/\sqrt{x}$ for $x > 0.02$.

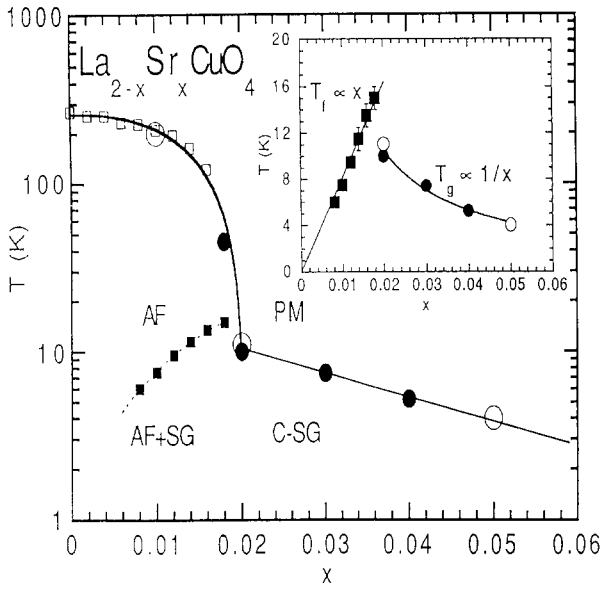

Fig. 8. Magnetic phase diagram of $La_{2-x}Sr_xCuO_4$. The inset shows linear plots of T_f and T_g versus x [29]. Abbreviations: PM, paramagnetic; AF, antiferromagnetic; SG, spin-glass; C-SG, cluster spin-glass.

From Fig. 8, an abrupt and distinct crossover at $x \approx 0.02$ occurs in the composition dependence of the freezing temperature: $T_f \alpha x$ for $x < 0.02$, whereas $T_g \alpha 1/x$ for $x > 0.02$. This novel behavior indicates that there is a crossover at $x \approx 0.02$ in the nature of the spin glass transition. As discussed above, for $x < 0.02$, the reentrant behavior below T_f should be viewed as the freezing of the spin degrees of freedom associated with the doped holes, superimposed on the pre-existing AF long range order. For $x > 0.02$, on the other hand, the system undergoes a collective phase transition from a paramagnetic state, with 2D dynamical correlations in undoped mesoscopic domains, to a cluster-spin-glass (C-SG) phase in which these domains freeze due to their mutual interaction; a static internal magnetic field occurs only below T_g [30].

3. Summary and conclusions

Using electrochemical oxidation of La_2CuO_4 at room temperature to form $La_2CuO_{4+\delta}$, two apparently distinct bulk superconducting phases are found at $\delta \lesssim 0.07$ ($T_c \approx 32$ K) and $\delta \gtrsim 0.08$ ($T_c \approx 45$ K); structural studies on powder and single crystal samples of these materials were carried out. Sr-doped compounds $La_{2-x}Sr_xCuO_{4+\delta}$ were also synthesized by electrochemical oxidation of ceramic $La_{2-x}Sr_xCuO_4$. Bulk superconductivity is found with onset $T_c \approx 40$ K for the whole range $0.01 \leqslant x \leqslant 0.15$ for maximally oxidized samples, whereas for $\delta = 0$, optimum superconductivity with $T_c \approx 38$ K only occurs for $x = 0.15$–0.20. Magnetic susceptibility and iodometric titration experiments indicate that the hole doping levels in the CuO_2 planes of $La_2CuO_{4.11}$ and $La_{1.92}Sr_{0.08}CuO_{4.07}$ are nearly identical with each other and with that of conventionally prepared $La_{1.85}Sr_{0.15}CuO_4$. For $\delta \approx 0.03$, macroscopic phase separation below ≈ 300 K into superconducting $La_{2-x}Sr_xCuO_{4+\delta'}$ ($\delta' \approx 0.07$) and nonsuperconducting $La_{2-x}Sr_xCuO_{4+\delta''}$ ($\delta'' \approx 0.00$) phases, known to occur for $x = 0$, disappears by $x \approx 0.03$.

The behaviors of the Néel temperature $T_N(x)$ and $\chi(x, T)$ of the antiferromagnetic phase ($0 \leqslant x \lesssim 0.02$, $\delta'' \approx 0.00$) reveal a novel microscopic segregation of the doped holes in this phase into walls of hole-rich material separating undoped domains. ^{139}La NQR measurements indicate that the spin degrees of freedom associated with the doped holes freeze below $T_f = (815\text{ K})x$, with $T_f(x = 0.02) \approx 16$ K; this spin-glass ordering is superimposed on the long-range AF order of the Cu spin system. For $x > 0.02$ where long-range AF order does not occur, the system undergoes a collective phase transition from a paramagnetic state, with 2D dynamical correlations in undoped mesoscopic domains, to a cluster-spin-glass phase in which these domains freeze due to their mutual interaction; a static internal magnetic field occurs only below T_g.

Acknowledgments

Ames Laboratory is operated for the US Department of Energy by Iowa State University under Contract No. W-7405-Eng-82. The work at Ames was supported by the Director for Energy Research, Office of Basic Energy Sciences. The work at Argonne National Laboratory was supported by the US Department of Energy under Contract No. W-31-109-Eng-38 (JDJ, AJS) and by the National Science Foundation Office of Science and Technology Centers Grant No. DMR-91-20000 (PGR, JLW).

References

1 J. Beille, R. Cabanel, C. Chaillout, B. Chevalier, G. Demazeau, F. Deslandes, J. Etourneau, P. Lejay, C. Michel, J. Provost, B. Raveau, A. Sulpice, J.-L. Tholence and R. Tournier, *C.R. Acad. Sci. (Paris), 304* (1987) 1097.

2 J.D. Jorgensen, B. Dabrowski, S. Pei, D.G. Hinks, L. Soderholm, B. Morosin, J.E. Schirber, E.L. Venturini and D.S. Ginley, *Phys. Rev. B, 38* (1988) 11337 and refs. therein.

3 C. Chaillout, S.W. Cheong, Z. Fisk, M.S. Lehmann, M. Marezio, B. Morosin and J.E. Schirber, *Physica C, 158* (1989) 183.

4 P. Zolliker, D.E. Cox, J.B. Parise, E.M. McCarron III and W.E. Farneth, *Phys. Rev. B, 42* (1990) 6332.

5 J.D. Jorgensen, H. Shaked, D.G. Hinks, B. Dabrowski, B.W. Veal, A.P. Paulikas, L.J. Nowicki, G.W. Crabtree, W.K. Kwok, L.H. Nunez and H. Claus, *Physica C, 153–155* (1988) 578.

6 R. Yoshizaki, N. Ishikawa, M. Adajatsu, J. Fujikami, H. Kurahashi, Y. Saito, Y. Abe and H. Ikeda, *Physica C, 156* (1988) 297.
7 E.J. Ansaldo, J.H. Brewer, T.M. Riseman, J.E. Schirber, E.L. Venturini, B. Morosin, D.S. Ginley and B. Sternlieb, *Phys. Rev. B, 40* (1989) 2555.
8 M.F. Hundley, J.D. Thompson, S.-W. Cheong, Z. Fisk and J.E. Schirber, *Phys. Rev. B, 41* (1990) 4062.
9 P.C. Hammel, A.P. Reyes, Z. Fisk, M. Takigawa, J.D. Thompson, R.H. Heffner, S.-W. Cheong and J.E. Schirber, *Phys. Rev. B, 42* (1990) 6781.
10 K.-I. Ueda, T. Sugata, Y. Kohori, T. Kohara, Y. Oda, M. Yamada, S. Kashiwai and M. Motoyama, *Solid State Commun., 73* (1990) 49.
11 L.L. Miller, K. Sun, D.C. Johnston, J.E. Schirber and Z. Fisk, *J. Alloys Comp., 183* (1992) 312.
12 C. Chaillout, J. Chenavas, S.-W. Cheong, Z. Fisk, M. Marezio and B. Morosin, *Physica C, 170* (1990) 87.
13 A. Wattiaux, J.C. Park, J.C. Grenier and M. Pouchard, *C.R. Acad. Sci. (Paris), 310* (1990) 1047.
14 J.C. Grenier, A. Wattiaux, N. Lagueyte, J.C. Park, E. Marquestaut, J. Etourneau and M. Pouchard, *Physica C, 173* (1991) 139.
15 J.C. Grenier, A. Wattiaux, J.P. Doumerc, P. Dordor, L. Fournes, J.P. Chaminade and M. Pouchard, *J. Solid State Chem., 96* (1992) 20.
16 J.C. Grenier, N. Lagueyte, A. Wattiaux, J.-P. Doumerc, P. Dordor, J. Etourneau and M. Pouchard, *Physica C, 202* (1992) 209.
17 J.C. Grenier, A. Wattiaux and M. Pouchard, in K.A. Müller and G. Benedek (eds.), *Phase Separation in Cuprate Superconductors*, World Scientific, Singapore, 1993, pp. 187–207.
18 F.C. Chou, J.H. Cho and D.C. Johnston, *Physica C, 197* (1992) 303.
19 V.J. Emery, S.A. Kivelson and H.Q. Lin, *Phys. Rev. Lett., 64* (1990) 475.
20 V.J. Emery and S.A. Kivelson, in K.A. Müller and G. Benedek (eds.), *Phase Separation in Cuprate Superconductors*, World Scientific, Singapore, 1993, pp. 1–16; *Physica C, 209* (1993) 597.
21 D. Vaknin, J.L. Zarestky, D.C. Johnston, J.E. Schirber and Z. Fisk, *Phys. Rev. B,* to be published.
22 F.C. Chou, D.C. Johnston, S.-W. Cheong and P.C. Canfield, *Physica C, 216* (1993) 66.
23 P.G. Radaelli, J.D. Jorgensen, A.J. Schultz, B.A. Hunter, J.L. Wagner, F.C. Chou and D.C. Johnston, *Phys. Rev. B, 48* (1993) 499.
24 E. Takayama-Muromachi, T. Sasaki and Y. Matsui, *Physica C, 197* (1993) 97.
25 J.H. Cho, F.C. Chou and D.C. Johnston, *Phys. Rev. Lett., 70* (1993) 222.
26 T. Thio, T.R. Thurston, N.W. Preyer, P.J. Picone, M.A. Kastner, H.P. Jenssen, D.R. Gabbe, C.Y. Chen, R.J. Birgeneau and A. Aharony, *Phys. Rev. B, 38* (1988) 905.
27 D.C. Johnston, S.K. Sinha, A.J. Jacobson and J.M. Newsam, *Physica C, 153–155* (1988) 572.
28 For a review, see D.C. Johnston, *J. Magn. Magn. Mater., 100* (1991) 218.
29 F.C. Chou, F. Borsa, J.H. Cho, D.C. Johnston, A. Lascialfari, D.R. Torgeson and J. Ziolo, *Phys. Rev. Lett., 71* (1993) 2323.
30 J.H. Cho, F. Borsa, D.C. Johnston and D.R. Torgeson, *Phys. Rev. B, 46* (1992) 3179.
31 R.J. Birgeneau and G. Shirane, in D.M. Ginsberg (ed.), *Physical Properties of High Temperature Superconductors I*, World Scientific, Singapore, 1989, pp. 151–211.